THE UNIVERSITY OF
NEW SOUTH WALES

**SCHOOL OF ELECTRICAL ENGINEERING
AND TELECOMMUNICATION**

Refined Algorithm for Frequency Estimation of A Real Sinusoid in Smart Grid

by

Qipeng Liu

Thesis submitted as a requirement for the degree

Bachelor of Engineering (Electrical Engineering)

Submitted: October 26, 2015
Supervisor: Elias Aboutanios

Student ID: z3372038
Topic ID: EAB23

Abstract

In this thesis report, a novel efficient algorithm for the smart grid is proposed to estimate the frequency of a real sinusoidal signal with additive white Gaussian noise. This method modifies the dichotomous search estimator for complex exponential signal model to fit the real sinusoidal signal model, which considers and calculates the spectral leakage based on the original interpolation on Fourier coefficients. Simulation result are also shown to prove the proposed algorithm could generate more accurate frequency estimation in various signal-to-noise(SNR) situations, tested frequency and phase shift of the signal. The root-mean-squared-error(RMSE) of the simulated results performs similar results as the Cramer-Rao Lower Bound(CRLB) with sufficient iterative processes.

Abbreviations

AMDS Aboutanios's Modified Dichotomous Search

AWGN Additive White Gaussian Noise

CRLB Cramer-Rao Lower Bound

DFT Discrete Fourier Transform

ESPRIT Estimation of Signal Parameters Via Rotational Invariant Techniques

FFT Fast Fourier Transform

MLE Maximum Likelihood Estimation

MUSIC Mutiple Signal Classification

RMSE Root Mean Square Error

SNR Signal to Noise Ratio

SVD Singular Value Decomposition

Contents

Chapter 1

Introduction

1.1 Context

The smart grid uses signal processing and communication techniques for the power grid in order to detect and react to the changes in usage. Accurate frequency estimations are the prerequisite of the functional smart grid to maintain stability for the whole system.[1]. Unexpected frequency variations from the nominal value generate unstable system situations, including voltage sags and generator-load mismatches which transmit and accumulate rapidly[2]. Thus, the accurate frequency tracking with fast responses becomes one of the most important considerations to support the smart grid[3].

As the waveform for each phase of voltage in the smart grid is shown as a single-phase real sinusoid, designing a robust algorithm for the single phase frequency estimation is classical yet important research problem in digital signal processing. Comparing with complex exponential signal model, the frequency estimation of a real sinusoidal model is more complicated in providing satisfying accuracy. Existed methods of frequency estimation for the sinusoidal signal are incompetent for fast frequency tracking. For the algorithms using subspace methods in time domain, they used the MUltiple SIgnal Classification(MUSIC)[4] combining with Estimation of Signal Parameters via Rotational Invariant Techniques(ESPRIT)[5] and Matrix Pencils[6]. These algorithms generate the accurate frequency estimation, whereas they suffer from the computational inefficiency

due to large number of calculations in Singular Value Decomposition(SVD) and matrix inversion process. The algorithm based on maximum likelihood estimations(MLE) in frequency domain, on the other hand, are more popular for research and industrial purposes because of the lower demand of computations. The usage of Fast Fourier Transform(FFT) followed with interpolations by single point Discrete Fourier Transform(DFT) generates the outstanding estimation for complex exponential signals with satisfying computational speed[8]. However, due to spectral leakage effect, algorithms based on MLE result in biased estimations for real sinusoidal signals, which lead indispensable deviations from anticipated true frequencies[10]. To solve such problems, multiple window functions were designed from previous researches to reduce the effects of spectral leakage. However, window functions increase the sensitivity of noise and degrade the performance by sacrificing the overall estimating accuracy[11].

1.2 Problem Statement

Design or refine an algorithm of frequency estimation which is fit to fast frequency tracking for the smart grid. This algorithm is required to analyse the model of a real sinusoidal with additive white Gaussian noise. To support the fast frequency tracking, the computational complexity should be reduced to the minimum. The algorithm need provide sufficient accuracy as well, which means the estimating variance should follow the benchmark of CRLB closely.

1.3 Outline

In this thesis report, a refined iterative algorithm is presented in frequency domain which gives unbiased accurate frequency estimation without using window functions. The dichotomous search given by Aboutanios[9] is refined by adding more procedures to eliminate the effects from spectral leakage iteratively. The simulated results show the estimating variance sitting on the benchmark of Cramer-Rao Lower Bound(CRLB) for only several iterations, which makes the estimating process efficient in computational costs.

Chapter 2 shows the background knowledge for frequency estimation of a real sinusoidal signal. It includes the demonstration of signal model, MLE theory, Fourier Transforms, estimating deviations and Cramer-Rao Lower Bound. Chapter 3 states the existed methods of single phase frequency estimation, consisting of Matrix Pencil and interpolations with window functions. Chapter 4 demonstrates the refined algorithm based on the AMDS, introducing procedures and explanations of the process. Chapter 5 presents the simulated results to verify the efficiency of the proposed algorithm by comparing RMSE with CRLB and other algorithms. Chapter 6 gives out the conclusion and the potential improvements for the future works.

Chapter 2

Background

The background knowledge is introduced in this chapter, which is helpful to lead the concepts of frequency estimation more comprehensive.

2.1 Signal Model

The signal in the smart grid has its specific characteristics. The voltage wave in the grid is periodic and the frequency is single tone with approximate value of 50 Hz. Moreover, the data used in the frequency estimator is often combined with noise, such as environmental noise. The signal is sampled to be discrete signal with sufficient sampling frequency f_s. Thus, the sampled periodic single-tone model combining with the noise in research is shown as equation (2.1)[12].

$$x[n] = s[n] + w_r[n] \tag{2.1}$$

s[n] is the signal term, which the frequency is required to be determined. We assume that the signal is sampled within a small period and the frequency is stable in these samples. If s[n] is a complex exponential signal, the mathematical representation is shown as equation (2.2),

$$s[n] = Ae^{j2\pi\frac{f}{f_s}n+\phi} \tag{2.2}$$

where ϕ, A and f denote the initial phase shift, the amplitude and the true frequency respectively. For the case of single phase sinusoidal signal in the real grid, the signal is

modeled as equation (2.3),

$$\begin{aligned} s[n] &= Acos(2\pi\frac{f}{f_s}n + \phi) \\ &= Acos(2\pi f_a n + \phi) \end{aligned} \tag{2.3}$$

where for simplicity, f_a represents the normalised frequency in the range $[0, 0.5]$. For the noise term $w[n]$, both unbiased and biased noise source could be added into the signal. Biased noise is treated as the disturbance from another power with certain frequency. Because of limited resources and time for the research, the case for biased noise is not considered in this research. For simulating the unbiased random noise, it has developed a suitable mathematical model called Additive White Gaussian Noise(AWGN), which shows in the equation (2.4).

$$w[n] = \frac{1}{\sqrt{2\pi\sigma^2}}e^{-\frac{(x-\mu)^2}{2\sigma^2}}; \tag{2.4}$$

where μ is the mean of the noise and σ is the square-root of variance for the noise. For unbiased white noise, the mean should be zero and the variance is uniform which is equal to the power density and related to the SNR ratio. Note that the SNR is obtained from:

$$\rho = \frac{\text{Signal Power}}{\text{Noise Power}} \tag{2.5}$$

The signal power for the exponential complex signal is A^2 and the signal power for the sinusoidal signal is $\frac{A^2}{2}$. SNR is usually measured in the basis of dB, thus for the SNR of the sinusoidal signal:

$$\rho = \frac{|A|^2}{2\sigma^2} = 10\log_{10}(\frac{|A|^2}{2\sigma^2})(dB) \tag{2.6}$$

2.2 MLE Theory

Maximum Likelihood Estimation(MLE) is extensively used in analyzing the statistical problems. It is defined as, for a given statistical model, MLE estimation provides the parameters that could maximize the likelihood function of an observer[13]. For the mathematical representation of MLE algorithm, the equation is shown as equation (2.7),

$$L(x|\hat{\theta}_{ML}) = \sup_{\theta} L(x|\theta) \tag{2.7}$$

where x denotes an observation of system X and θ represents the related parameters of the given system. The MLE estimator then constructs the likelihood function $L(x|\theta)$ and search the parameters $\hat{\theta}_{ML}$ in maximizing the possibilities.

In the aspects of frequency estimation, maximum likelihood estimator could be explained as, given a block of N samples, the estimation of the frequency could maximize the possibility in obtaining the actual N number of samples when the measurements have been made.[14] The specific formula is given by:

$$\hat{f}_{ML} = \arg_{\lambda} \max I(\lambda) \tag{2.8}$$

2.3 Fourier Transform

Performing as an efficient method of MLE in frequency estimation, Fourier Transform is mostly used to project the data in time domain to frequency domain. The location which obtains the maximum amplitude in frequency spectrum, shows the highest probability that this frequency is the parameter of the data. The process of Fourier Transform for sampled data, called Discrete Fourier Transform(DFT), is shown as equation (2.9).

$$X[k] = \sum_{k=0}^{N-1} x[n] e^{-j2\pi k \frac{n}{N}} \tag{2.9}$$

The Fourier transform of an exponential complex signal is then calculated by linearity theorem[15][16], shown as equation (2.10).

$$e^{i2\pi ax} f(x) \Longrightarrow \breve{f}(\xi - a) \tag{2.10}$$

As the signal is sampled in the limited time,

$$f(x) = \begin{cases} 1 & \text{when x} \leq \tau \\ 0 & \text{when x} > \tau \end{cases} \tag{2.11}$$

the Fourier Transform of $f(x)$ is shown as equation (2.12).

$$F(f(x)) = \tau sinc(\tau\pi f) \tag{2.12}$$

$$e^{i2\pi f_a x} f(x) \Longrightarrow \tau sinc(\tau\pi(f - f_a)) \tag{2.13}$$

Thus, the sampled signal of complex exponential model shows as a sinc function in the spectrum and the function is shifted to the positive direction with the length of true frequency f_a. Meanwhile, for the case of a real sinusoidal by using the linearity, the equation is shown below.

$$cos(2\pi ax) f(x) \Longrightarrow 0.5\breve{f}(\xi - a) + 0.5\breve{f}(\xi + a) \tag{2.14}$$

Substitute $f(x)$ with equation (2.11), the result of Fourier Transform is shown as equation (2.15).

$$cos(2\pi f_a x) f(x) \Longrightarrow 0.5\tau sinc(\tau\pi(f - f_a)) + 0.5\tau sinc(\tau\pi(f + f_a)) \tag{2.15}$$

It appears two sinc functions at the location of f and $-f$. As the tail of the sinc function at $-f$ affects the shape of the sinc function at f, the MLE estimator in searching maximum amplitudes generates biased result and degrades the overall accuracy.

Overall, searching frequency with the peak amplitude estimates the true frequency. For simplicity, the frequency estimation consists of two processes, including coarse estimation and refined estimation. Coarse estimation is using Fast Fourier Transform(FFT) to locate the rough frequency in the maximum bin approximately and refined estimation uses interpolations such as dichotomous search and zero-paddings to shrink the size of maximum bin to increase the resolution.

2.4 Estimating Deviations

The MLE algorithms always provide the estimated frequency with errors. The performance of an estimator could be determined by calculating the root-mean-squared-error(RMSE) after implementing a large number of experiments. The RMSE formula is shown in equation (2.16).

$$\text{RMSE} = \sqrt{\frac{\sum_{i=1}^{N}(f_{est} - f_{true})^2}{N}} \tag{2.16}$$

For testing the frequency estimator in this research, 1000 times simulations were performed in a single point of SNR. This number is calculated by the statistics as less experiments cause inaccuracy for average RMSE, while more experiments cause the large computational stress for the machine.

The factors influencing the overall estimating performance for the real grid could be summarized into three main aspects, including the environmental noise, lack of the axis resolution and the spectral leakage.

2.4.1 Environmental Noise

The additive white noise is the prime element in generating the deviations. The noise power is uniformly distributed in the frequency spectrum and related to SNR which is already shown in equation (2.6). When SNR is smaller than the threshold point and signal peaks are fully concealed by the noise power, the largest peak in the spectrum could be everywhere inside the range of sampling frequency which is unrelated to the signal. Then the estimating variance dramatically increases which indicates the estimator is unreliable. This is called an outlier situation, which is not the circumstance in my research.

When the SNR is larger than the threshold point, the white noise still draws the effects in reducing the overall estimating performance, although the influence is smaller than the outlier cases. It causes slight deviations, but the estimation still follows the signal in the maximum bin. White noise is unable to be fully eliminated, thus in each SNR situation,

the best estimating performance is calculated as Cramer-Rao Lower Bound(CRLB) in statistics, which is shown in the following section.

2.4.2 Lack of Resolution

As the true frequency is a statistically random number, the estimated frequency is not exactly equal to this number. The MLE estimator determines the maximum bin where the true frequency is inside. For coarse estimation by using Fast Fourier Transform(FFT), the resolution is only related to the number of sampling points for normalised frequencies. The resolution unit is shown as equation (2.17):

$$\delta = \frac{1}{N_{fft}} \tag{2.17}$$

With interpolations, the resolution unit δ is decreased further. As the true frequency in the maximum bin show as uniform distribution, the estimating variance by resolution is shown as equation (2.18).

$$Var = \frac{\delta^2}{12} \tag{2.18}$$

2.4.3 Spectral Leakage

From equation (2.15), there are two sinc functions at both f and $-f$ in the frequency spectrum of a real sinusoid. One sinc function affects the overall shape of the other sinc function, which generates the bias at the peak amplitude. Figure 2.1 explains the spectral leakage effect, shown below.

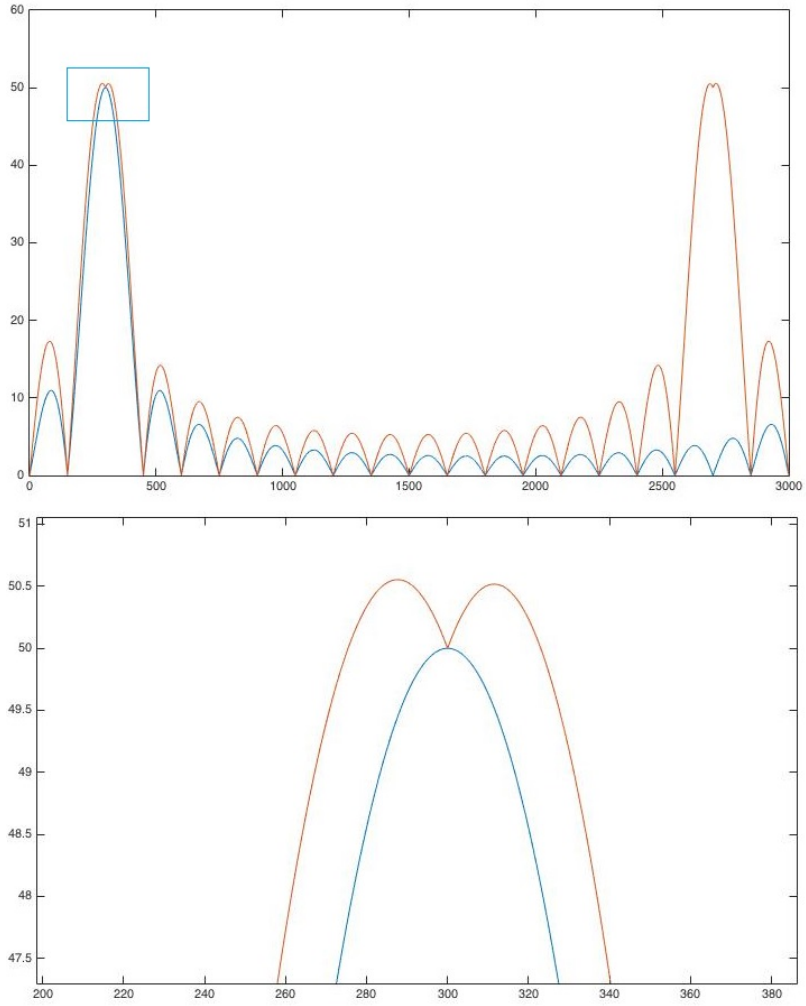

Figure 2.1: Spectral Leakage Effect in Frequency Spectrum

From the graph, the red line denotes the real sinusoidal signal and blue line shows the complex exponential signal in frequency spectrum. Due to the aliasing effect, the spectrum with frequency $[-0.5, 0]$ is shifted to the right at $[0.5, 1]$. Whereas two signals have the same frequency, the peak locations are different in frequency spectrum. Due to spectral leakage, the estimated frequency of a real sinusoid has large deviations shown in

the graph. This is the main weakness in using the exponential frequency estimator and measuring the real sinusoidal model.

2.5 Cramer-Rao Lower Bound

Cramer-Rao Lower Bound(CRLB) is usually utilised as the benchmark to verify the performance of a frequency estimator. It is defined as the theoretically lowest estimating variance in statistics for all frequency estimators without outliers. It is derived by performing diagonalization of the inverted Fisher information matrix assuming that the MLE estimator is unbiased. The bound for a complex exponential signal is initially proposed by Rife[17], as when neither the phase nor the amplitude is known, the CRLB is expressed as equation shown below.

$$\text{CRLB} = \frac{3\sigma^2}{2\pi^2 A^2 N(N^2-1)} \leq var(\hat{f} - f) \tag{2.19}$$

The process to calculate the CRLB for a real sinusoidal is similar with the complex exponential one. The specific procedures is mentioned in [18], [19] and [20], related to the inversion of Fisher information matrix as well. There is no simpler representation of this CRLB, thus the specific procedures for a real sinusoid are omitted in this part.

2.6 Research Objectives

The main idea for thesis research is to design or refine an frequency estimation algorithm for a real sinusoid for the smart grid. It is divided into three objectives:

1. **Basic Objective**: Evaluating existed methods of frequency estimation for a real sinusoid in theory and simulation.

2. **Advanced Objective**: Design an alternative method of frequency estimation for the same purpose.

3. **Final Objective**: Show that the alternative method has better performance than existed methods in simulation and in the real grid.

Chapter 3

Literature Review for Existed Methods

3.1 Matrix Pencil Method

Matrix Pencil Method is one of the most representative frequency estimators based on time domain. It is proposed by Hua and Sarkar in [6] and also mentioned in [7]. It is initially used for multiple complex exponential signals. In this research, it works functionally for a real sinusoid as well, because as mentioned in Euler's Theorem, a real sinusoid is composed by two exponential signals. As it is working in time domain and is different from MLE estimators, it is not influenced by spectral leakage and lack of resolution problem.

3.1.1 Working Principal

The signal $x[n]$ can be represented as equation (3.1) with no damping.

$$x[n] = s[n] + w_r n = \sum_{i=1}^{M} |a_i| e^{j\theta_i} e^{(j2\pi f_i)n} + w_r[n] \tag{3.1}$$

where $|a_i|e^{j\theta_i}$ is called complex amplitude and $e^{(j2\pi f_i)n}$ is named as signal pole. Assuming the signal is sampled as $x[n]$ with length N, two matrices are constructed as equation

(3.2) and (3.3).

$$\mathbf{X}_0 = \begin{bmatrix} x_{L-1} & x_{L-2} & \dots & x_0 \\ x_L & x_{L-1} & \dots & x_1 \\ \vdots & \vdots & \ddots & \vdots \\ x_{N-2} & x_{N-3} & \dots & x_{N-L-1} \end{bmatrix}. \tag{3.2}$$

$$\mathbf{X}_1 = \begin{bmatrix} x_L & x_L & \dots & x_1 \\ x_{L+1} & x_L & \dots & x_2 \\ \vdots & \vdots & \ddots & \vdots \\ x_{N-1} & x_{N-2} & \dots & x_{N-L} \end{bmatrix}. \tag{3.3}$$

where L denotes the pencil parameter. These matrices can be decomposed as:

$$\mathbf{X}_0 = Z_L B Z_R, \quad \mathbf{X}_1 = Z_L B Z Z_R \tag{3.4}$$

where Z_L and Z_R are Vandermonde matrices, and B and Z are diagonal matrices generated from the complex amplitude and signal poles respectively. Considering the equation (3.4):

$$\mathbf{X}_1 - \lambda \mathbf{X}_0 = Z_L B (Z - \lambda I) Z_R \tag{3.5}$$

where $\mathbf{X}_1 - \lambda \mathbf{X}_0$ and $Z - \lambda I$ has the rank of $M - P$ and P represents the number of poles. The number of poles is related to the number of frequencies in the data, which fits:

$$\mathbf{X}_1 q_i = e^{(j2\pi f_i)n} \mathbf{X}_0 q_i \tag{3.6}$$

In equation (3.6), $e^{(j2\pi f_i)n}$ and q_i represent each eigenvalue with unique frequency and opposite eigenvector respectively. Thus, by using SVD with matrix diagonalization and matrix inversion to equation (3.5), correct amount of signal poles and estimated frequency parameters are obtained by matrix pencil algorithm.

3.1.2 Estimator Performance

The proposed estimating variance exactly follows the CRLB after threshold point. In simulation, the frequency is set to around 0.0125 and the number of samples is set to 80. The signals all have unity amplitude and no initial phase shift. The simulated result is shown as Figure 3.1. From the graph, the performance for Matrix Pencil is

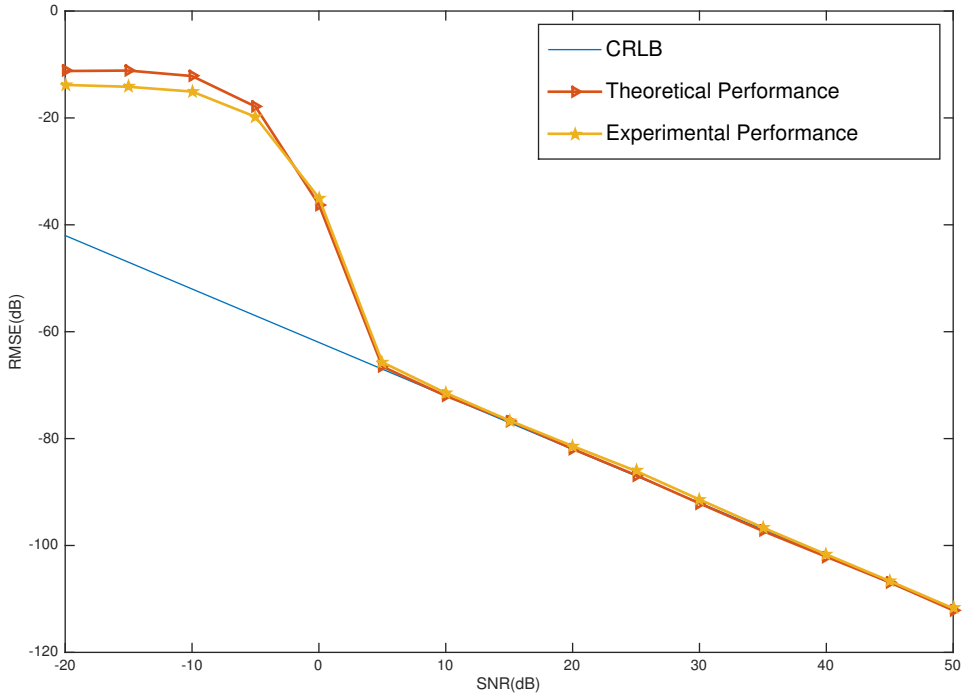

Figure 3.1: Simulated Result for Matrix Pencil Method

satisfying in accuracy as for any SNR larger than threshold point, the RMSE follows CRLB closely. However, due to large amount of calculations in SVD and matrix inversion which is associated with $O(N^3)$, the computational complexity is the main concern in using Matrix Pencil Algorithm for fast frequency tracking of the smart grid.

3.1.3 Summary

1. **Advantage**: Highest accuracy following CRLB for any SNR larger than threshold point

2. **Disadvantage**: Complex in calculations and high computational stress

3.2 Window Functions with Intepolations

Window functions with intepolations are classical frequency estimating algorithm used for a real sinusoid based on MLE estimators. A window function defines a closed mathematics interval, with remaining zero value outside this interval. In signal processing, because of experimental restricts, the signal could only be sampled within the limited time period, or in other words, view through the window in the limited interval. In the time domain, the window function mostly shows the symmetric,non-negative and bell-shaped curves[21].The curve also could appear as the rectangle shape or the triangular shape.

3.2.1 Working Principal

Every window shows the sinc function in the frequency spectrum, consisting of the main lobe and the side lobes. If the window makes no changes on the sampled signal, there is a unit amplitude gain everywhere inside the window, which is a rectangular window. The opposite equations for rectangular windows are shown previously as equation (2.11) and equation (2.12), in both time domain and frequency domain. The graph of time-domain and frequency-domain for rectangular window is shown below as Figure 3.2. From the

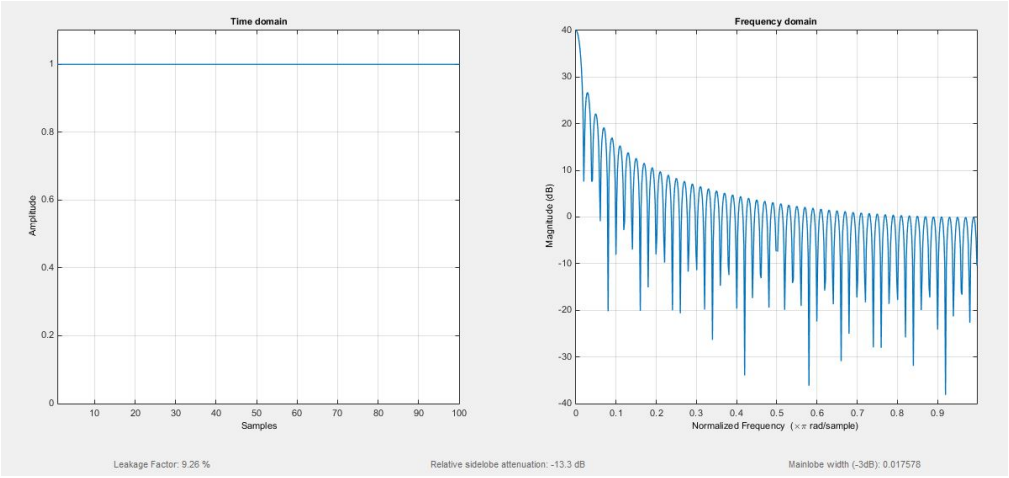

Figure 3.2: Rectangular Window: Time domain and Frequency Domain

graph, the bandwidth of the main lobe is very small and the gain for the side lobe is large enough to generate biased result due to spectral leakage. The bandwidth for the main lobe

is directly related to the sensitivity of additive noise, as the large-bandwidth main lobe attenuates the shape of peak point in the frequency spectrum, then the identical noise will cause more effects. The amplitude of the side lobes is related to the maximum accuracy which the estimator could obtain in the circumstances of high SNR. For any window functions, the bandwidth of main lobe is always inverse proportional to the amplitude of side lobes. Thus, the window function method is not a perfect solution to eliminate the error totally, as it decreases the spectral leakage effect while compromising the overall estimating performance. For the rectangular window, because of the small bandwidth in the main lobe and large amplitude in side lobes, the gap between the Cramer-Rao Lower Bound and the curve is small and the minimum estimating variance is excessive due to large spectral leakage. Meanwhile, window functions uses MLE estimators with interpolations to eliminate the lack of resolution problem. The procedure in using winodw functions is simply substituting window function into $f(x)$ then applying for MLE estimators.

Harris made a developed research on various window functions[22]. To review this method, some specific window functions will be tested in this section to compare the performance.

3.2.2 4th order B-Spline Window – Parzen Window

The mth order B-spline function could be defined by the recurrence formulas[23] in the limited time-interval:

$$w_1(t) = \begin{cases} 1 & \text{if } |t| < T/2 \\ 0 & \text{if } |t| \geq T/2 \end{cases} \tag{3.7}$$

The recurrence could be modified as the integral shown in the following function:

$$w_m(t) = \int_{-\infty}^{\infty} w_1(m\tau) w_{m-1}(\frac{m}{m-1}(y-\tau))d\tau, m = 2, 3, 4, ... \tag{3.8}$$

After solving the formula[24]:

$$w_m(t) = m^m \sum_{p=0}^{m} \frac{(-1)^p (t - (p - \frac{m}{2})\frac{T}{m})_+^{m-1}}{p!(m-p)!}, m = 1, 2, 3, ... \tag{3.9}$$

where:

$$(t-a)_+^{m-1} = \begin{cases} (t-a)^{m-1} & \text{if } t > a \\ 0 & \text{if } t \leq a \end{cases} \tag{3.10}$$

The shape of the curve in the time domain will be more similarity to the bell shape as m increases. In the frequency spectrum, the bandwidth of the main lobe is larger and the amplitude of side lobes is smaller as m increases. When m equals to 4, the formula equals to:

$$w_4(t) = \begin{cases} 4T^3 \frac{1-6(2\frac{t}{T})^2(1-2\frac{|t|}{T})}{3} & \text{if } |t| < \frac{T}{4} \\ 8T^3 \frac{(1-2\frac{|t|}{T})^3}{3} & \text{if } \frac{T}{4} \leq |t| < T/2 \\ 0 & \text{if } \frac{T}{2} \leq |t| \end{cases} \tag{3.11}$$

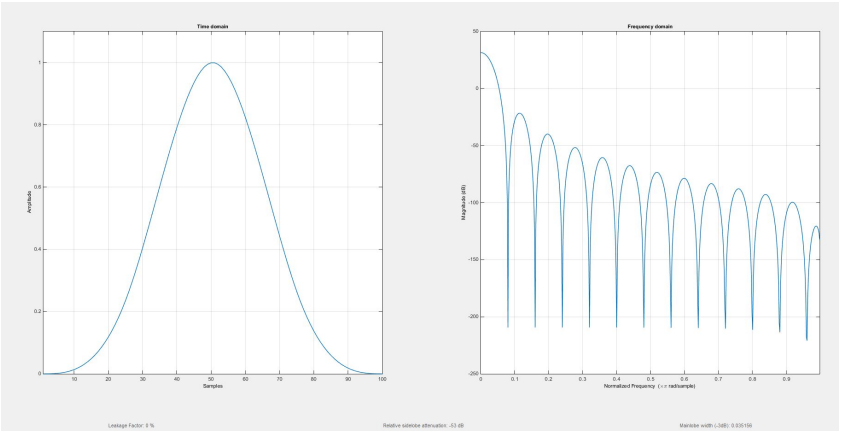

Figure 3.3: Parzen Window: Time domain and Frequency Domain

The shape for the Parzen Window in both time domain and frequency domain is shown in Figure 3.3. From the graph, the function in time domain forms a smooth bell-shaped curve. Moreover, the amplitude of side lobes is decreasing while the bandwidth in the main lobe is increasing, which means Parzen Window performs efficiently at very high SNR situation and lead low accuracy in the low SNR environment.

3.2.3 Hann(Hanning) Window

The generalized hamming windows are formed by the offset α and a one-cycle cosine wave with amplitude of β, the formula is shown below:

$$w(n) = \alpha - \beta cos(\frac{2\pi n}{N-1}); \tag{3.12}$$

Cosine tapering terms will reduce the amplitude of the side lobes, as the bandwidth of the main lobe will increase at the same moment[25]. Hann window is named by Julius von Hann, also called raised cosine window. It picks the average and same value to α and β at 0.5. Thus the formula is shown below:

$$w(n) = 0.5 - 0.5cos(\frac{2\pi n}{N-1}); \tag{3.13}$$

Thus, when n equals to 0 and $N-1$, the amplitude in time domain is zero. When n is equal to $\frac{N-1}{2}$, the amplitude in time domain shows the maximum value of 1. Figure 20 shows the time-domain spectrum and frequency spectrum. The main lobe bandwidth

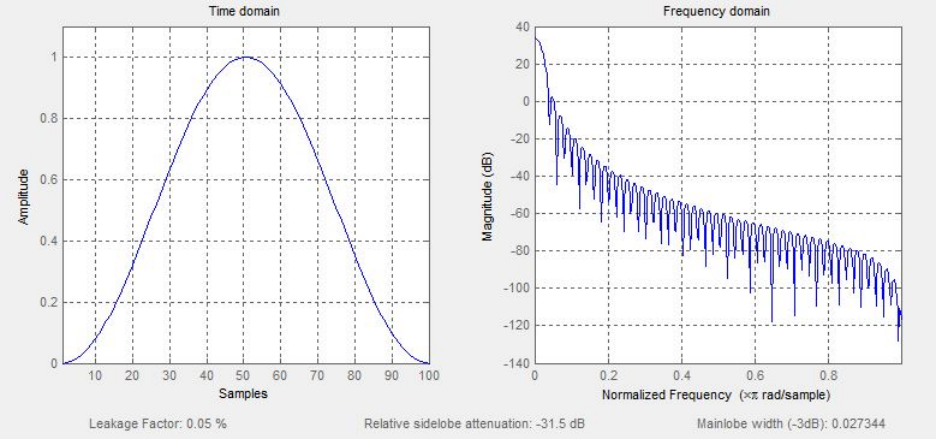

Figure 3.4: Hann Window: Time domain and Frequency Domain

is smaller than Parzen Window while the amplitude in the side lobes shows the reverse tendency.

3.2.4 Interpolation Methods

As MLE estimators suffer from lack of resolutions, the interpolation methods are proposed to reduce such problems. The simplest method to make interpolation is padding zeros into the data and then substituting into FFT peak detection. It is easy to implement, however, it consumes large computations in FFT transformation. As the reason that FFT costs the amount of calculations in $O(N \log_2 N)$, the number increases exponentially when zeros pad into the data. In this research, an efficient method is used to make interpolations, called Aboutanios's Modified Dichotomous Search(AMDS)[9].

The dichotomous search consists of two main processes, including coarse search and refining iterations. The maximum bin search by performing FFT generates the initial rough frequency estimation. It is a non-linear estimator and shows a threshold behaviour[26]. When SNR is smaller than the threshold, the occurrence of outliers appears frequently and estimating variance increases dramatically. The performance is largely degraded in this situation and we assume SNR is larger than threshold in the followings.

Zakhraov and Tozer initially proposed the binary narrowing method the locate the true maximum point. By comparing two FFT coefficients on both sides of the maximum point, a new maximum searching bin is obtained and the refined estimation is located at the centre of the new bin each cycle. Then the unit frequency is halved and the overall resolution is doubled.

Zakhraov and Tozer also found the requirements of 0.5 times zero-padding at the beginning of iterative process. Aboutanios explained the reason of the zero-padding prerequisite. As in the first iteration, the choice is made from either side of the maximum point. The FFT coefficients majorly depend on the effects of noise and after the first iteration, the estimating variance becomes:

$$\sigma_f{}^2 = \frac{0.25}{N^2} \tag{3.14}$$

The following iterations are mainly influenced by the first iteration. If an inaccurate choice is made in the first iteration, the error accumulates and is not recoverable by more iterations unless the true frequency is exactly located at the initial maximum point. Padding

Table 3.1: Aboutanios's Modified Dichotomous Search

Calculate	$S = FFT(s, L)$ and $Y(n) = \|S(N)\|^2$
Find	$m = \arg\max_n \{Y(n)\}$
Set	$\Delta = 0.75$,
	$Y_{-1} = Y(m-1), Y_0 = Y(m)$ and $Y_1 = Y(m+1)$
if	$Y_1 > Y_{-1}$
then	$Y_{-1} = \|\sum_{k=0}^{N-1} s(k) e^{-j2\pi \frac{k(m+1-2\Delta)}{N}}\|^2$ and $m = m + 1 - \Delta$
else	$Y_1 = \|\sum_{k=0}^{N-1} s(k) e^{-j2\pi \frac{k(m-1+2\Delta)}{N}}\|^2$ and $m = m - 1 + \Delta$
For I1 iterations do	
	$Y_0 = \|\sum_{k=0}^{N-1} x(k) e^{-j2\pi \frac{km}{L}}\|^2$ and $\Delta = \frac{\Delta}{2}$
	if $Y_1 > Y_{-1}$
	then $Y_{-1} = Y_0$ and $m = m + \Delta$
	else $Y_1 = Y_0$ and $m = m - \Delta$
Finally	$\hat{f} = \frac{m}{L}$

zeros into data array makes samples more densely and then eliminates the problem in first iteration. Aboutanios then proposed another method, shown in table 3.1, change the initial maximum point and the size of first searching bin. Although the first iteration has the probability in estimating to the wrong side, the modified dichotomous search has the opportunity to eliminate the error and recover the estimation to the correct side for more iterations.

Note that the variance for dichotomous searching algorithm equals to $\max(\text{CRLB}, {\sigma_f}^2)$ without considering spectral leakage effect, where ${\sigma_f}^2$ shows as equation (3.15).

$$ {\sigma_f}^2 = (\frac{1}{\sqrt{12} L 2^{Q-1}})^2 \tag{3.15} $$

I1 denotes the number of iterations and L equals to the length of FFT samples.

3.2.5 Simulated Result

We perform simulations to verify the performance of the estimating algorithm. In simulations, the frequency is set to around 0.0125 and the number of samples is set to 80. The signals all have unity amplitude and no initial phase shift. For both Parzen window and Hann window, 12 iterations were used in AMDS algorithm to increase the resolution. The simulated result is shown as Figure 3.5. The behaviour from the graph follows with the

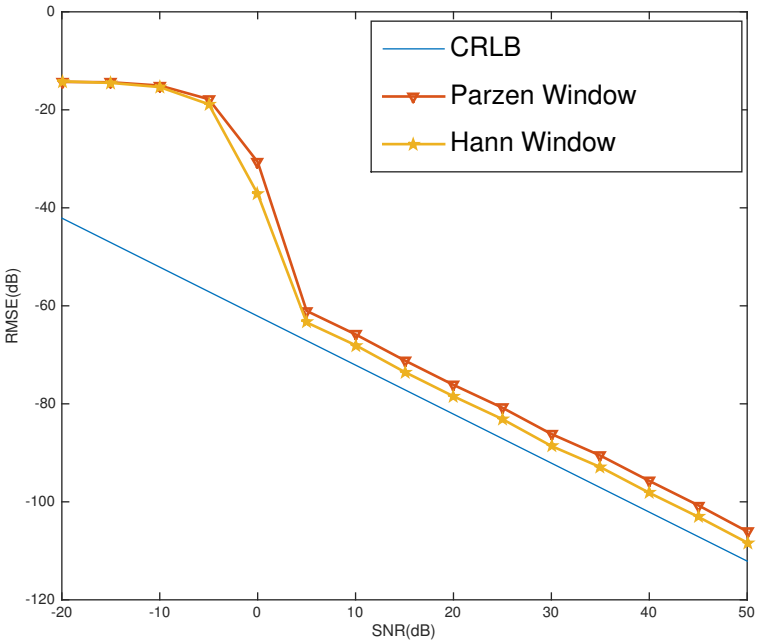

Figure 3.5: Simulated Result for Window Functions with Interpolations

theoretical results. As parzen window has more bandwith in main lobe comparing with Hann window, the estimating variance in small SNR is higher than Hann window. It is shown in the graph as the larger gap between the Parzen window and the CRLB. For the given SNR range larger than threshold point $[5, 60]$, both algorithms are not affected by the lack of resolution and spectral leakage effect. However, both algorithms are unable to follow the CRLB closely with an obvious gap which means window functions reduce the spectral leakage effects by sacrificing the overall estimating performance. From the

aspect of computational complexity, these algorithms consume less calculations which is only $O(N \log_2 N)$. Comparing with $O(N^3)$) for Matrix Pencil, it gives the faster response which is suitable for smart grid. However, the accuracy is the mainly concern for these algorithms.

3.2.6 Summary

1. **Advantage**: Easy to implement and computational efficiency.

2. **Disadvantage**: Overall performance is degraded and accuracy is not satisfactory.

Chapter 4

Refined Algorithm

The real sinusoidal signal is treated as the addition of two complex exponential signals with noise, shown as equation (4.1).

$$\begin{aligned} x(n) &= a\frac{e^{j\phi}}{2}e^{j2\pi fn} + a\frac{e^{-j\phi}}{2}e^{-j2\pi fn} + w_r(n) \\ &= A(f)e^{j2\pi fn} + A(f)^* e^{-j2\pi fn} + w_r(n) \\ &= s(n) + s^*(n) + w_r(n) \end{aligned} \tag{4.1}$$

AMDS algorithm works perfectly for exponential signal $s(n)$. If using dichotomous search directly to sinusoidal signal $x(n)$, the algorithm results in biased results due to the effects of $s^*(n)$. Thus, the refined estimator estimates and subtracts $s^*(n)$ from data in each iteration after each dichotomous search process. Thus, the whole estimation algorithm contains two separate iterations, I1 and I2, shown as the flow chart below.

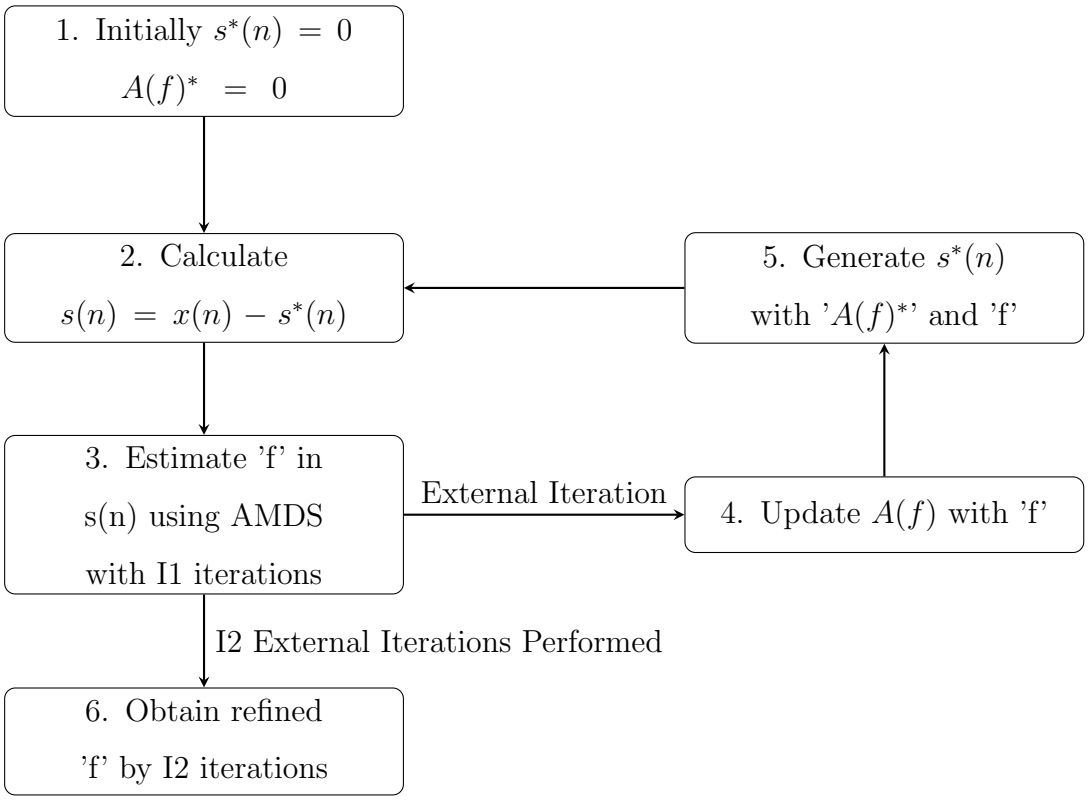

Table 4.1: Float Chart of Proposed Refined Algorithm

From the flow chart, I1 shows the internal iterations in AMDS. I2 consists the calculation of the parameters of $s^*(n)$, forming $s^*(n)$ in time domain and the subtraction from original data. s(n) is updated in each cycle of external iteration and $s^*(n)$ is mostly eliminated after several external iterations performed.

Then we explain the whole procedure in the fourth and fifth block shown in the flow chart. After the third block, the rough estimation of 'f' is obtained and the amplitude of that frequency in frequency domain is shown as equation (4.2),

$$A^T(f) = \sum_{n=0}^{N-1} s(k) e^{-j2\pi f \frac{n}{N}} \tag{4.2}$$

where $A^T(f)$ consists both true amplitude and spectral leakage, shown as equation (4.3).

$$A^T(f) = A(f) + A^*(f) \tag{4.3}$$

Thus, we need to calculate $A^*(f)$ to obtain A(f). $A^*(f)$ is generated from Fourier Trans-

form of $s^*(n)$ shown as equation (4.4).

$$\begin{aligned} A^*(f) &= \frac{1}{N}\sum_{n=0}^{N-1} s^*(n)e^{-j2\pi fn} \\ &= \frac{1}{N}\sum_{n=0}^{N-1} \hat{A(f)}^* e^{-j2\pi fn} e^{-j2\pi fn} \\ &= \frac{1}{N}\sum_{n=0}^{N-1} \hat{A(f)}^* e^{-j2\pi (2f)n} \quad \text{and by using power series theorem} \\ &= \frac{\hat{A(f)}^*}{N}\frac{1-e^{-j2\pi N(2f)}}{1-e^{-j2\pi(2f)}} \end{aligned} \tag{4.4}$$

where $\hat{A(f)}^*$ represents the conjugate of previous estimation of $A(f)$. Then new $A(f)$ is obtained from the subtraction of $A^T(f)$ and $A^*(f)$. We use the conjugate of new $A(f)$ to generate $s^*(n)$, which is shown in equation (4.5).

$$s^*(n) = A(f)^* e^{-j2\pi fn} \tag{4.5}$$

Thus, $s(n)$ is given out by subtracting $s^*(n)$ from $x(n)$, which is purely exponential

signal with no spectral leakage occurred in AMDS estimator. Significantly, the difference between $A^*(f)$ and $A(f)^*$ is that, $A^*(f)$ represents the small power of spectral leakage and $A(f)^*$ is simple conjugate of new amplitude estimation. Finally, the estimated frequency is refined and whole procedure for refined estimator is shown in table 4.2.

Table 4.2: Refined Estimator for Real Sinusoidal Signal

Set	$s^*(n) = zeros(1, N)$ and $A(f)^* = 0$
For I2 iterations do	
	$s(n) = x(n) - s^*(n)$
	$f = AMDS(s(n), \text{I1 iterations})$
	$A(f) = \sum_{n=0}^{N-1} s(k) e^{-j2\pi f \frac{n}{N}} - \frac{A(f)^*}{N} \frac{1-e^{-j2\pi N(2f)}}{1-e^{-j2\pi(2f)}}$
	$A(f)^* = conj(A(f))$
	$s^*(n) = A(f)^* e^{-j2\pi f n}$
Finally	Refined Frequency $= f$

Chapter 5

Simulated Results

5.1 Simulated Results

We show the simulated results by performing the refined estimator for real sinusoidal signal to verify the performance. In all simulations without special mentions, the test frequency is slightly varied around 0.0125 to avoid special integer values, which is also known as around 50Hz true frequency and 4000Hz sampling frequency for smart grid. N is fixed to be 80 and all amplitudes for test signals are set to be unity. For accuracy, all points in the graph are averaged from 1000 times experiments. The results are calculated as the Root-Mean-Squared-Error(RMSE), compared with CRLB to prove the efficiency.

5.2 Performance with Varying Phase Shift

In this test, we fix the SNR to 30dB. Iteration cycles are set to be 12 times and 8 times respectively. Note that in this situation, the CRLB plays the dominant role in limiting estimating variance, as the influence from the resolution is smaller than the effect from the noise.

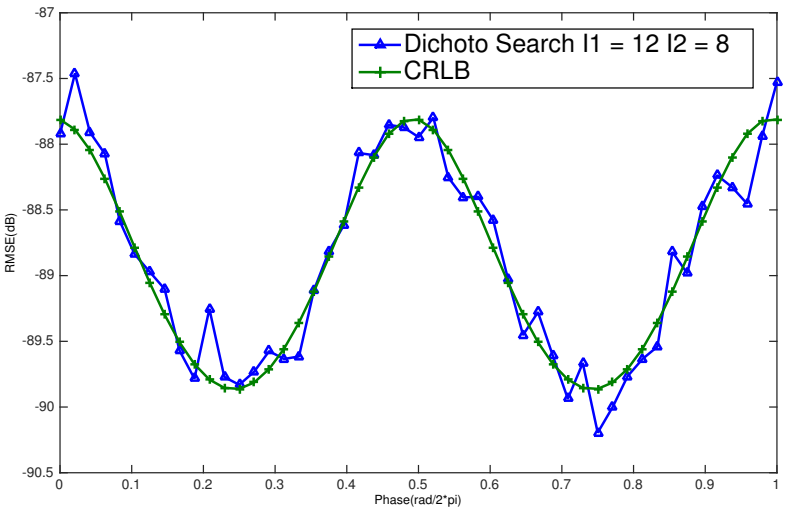

Figure 5.1: RMSE vs Phase Shift

From figure 5.1, we find that the proposed algorithm is well-performed with varying phase shift, as the experimental results from proposed algorithm is especially closed to theoretical CRLB. Although due to the limit number of experiments made, there are some little differences between experimental and theoretical results, which could be ignored. Meanwhile, the gap becomes larger when phase shift is closed to full cycle because of phase wrapping effect.

5.3 Performance with Varying Frequency

In this test, we fix the SNR to 30dB as well. Phase shift in every signal is set to be 0. Iterative cycles are set to be 12 times and 8 times respectively to provide the estimating variance limited by CRLB without influencing from resolution. As the frequency spectrum for real signal is periodic due to aliasing effects, the results are only concentrated in $f \in [0, 0.25]$. From figure 5.2, we find that both theoretical CRLB and real experimental

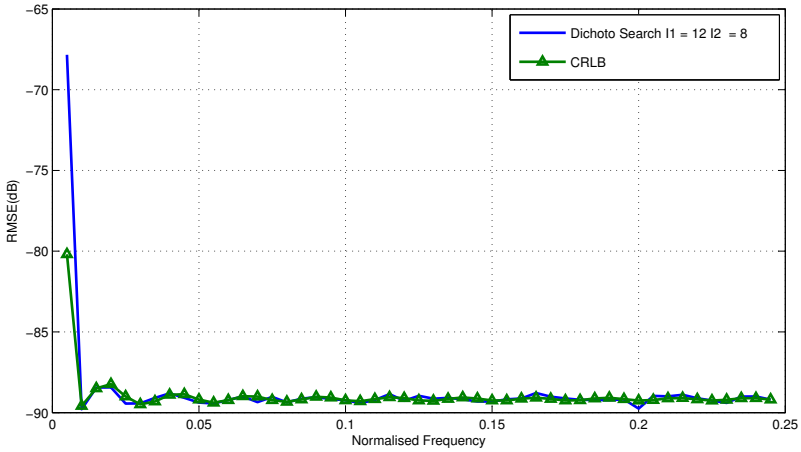

Figure 5.2: RMSE vs Frequency

RMSE become smooth as the normalised frequency is towards to 0.25. This is caused by the interference between two exponential signals. When true frequency is 0.25, the distance between two exponential signals turns into maximum and interference becomes minimum. When true frequency moves extremely close to 0, the interference and the estimating variance becomes larger as the main lobes of both sinc function overlap. In spite of the gap at the extreme small frequency, the refined frequency estimator works well for the frequency larger than around 0.01.

5.3.1 Performance with Varying SNR

Finally, we delete the initial phase shift in test signals and the frequency is fixed to 0.0125. In this test, we vary I1 or I2 separately while the other is fixed. Figure 5.3 shows the situation with varying I1 and fixed I2.

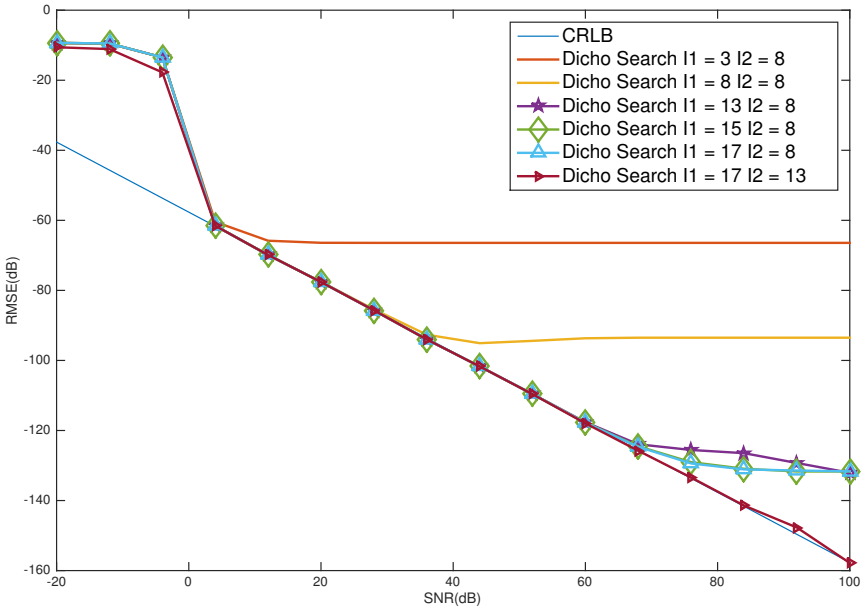

Figure 5.3: RMSE vs Varying I1 & Fixed I2

From the graph, it could be clearly seen that when I2 and SNR is large enough, increasing I1 will improve the overall estimating performance and display the RMSE close to CRLB. In this case, the overall resolution is limited by I1 and the variance is unable to decrease despite higher SNR provided. When I1 is large enough compared to fixed I2, such as the lines with I1 equal to 13, 15 and 17, the resolution then depends on I2. From the graph, those three lines ends on the same RMSE when SNR is too large. Increasing I2 continues decreasing the RMSE further, shown as the red line with right-triangle markers. The same approach is found when I1 is fixed and I2 is changing, shown

as Figure 5.4. From the graph, the situation is quite similar with the graph of fixed I2

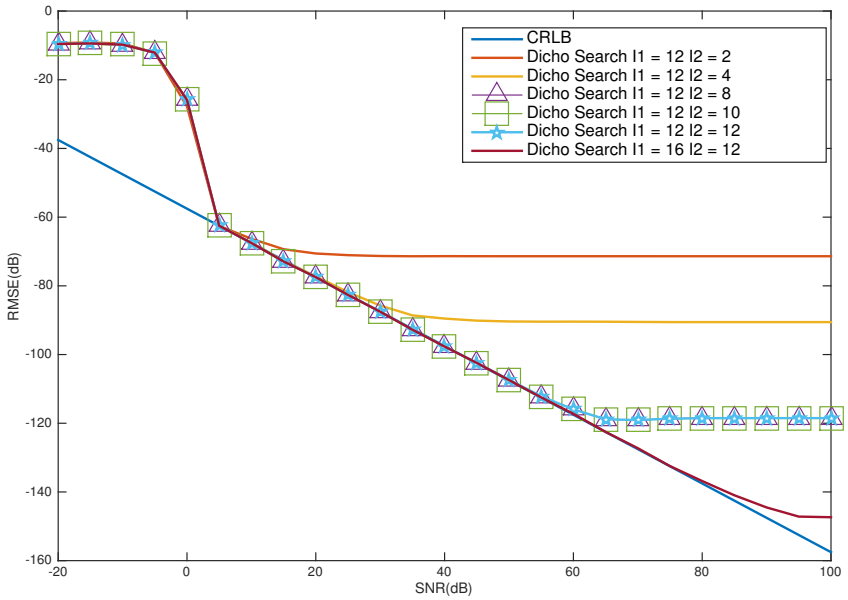

Figure 5.4: RMSE vs Varying I2 & Fixed I1

and varying I1. When I2 is large enough, the resolution is restricted by I1. When SNR is small, the result follows with CRLB perfectly. When resolution is smaller than the CRLB, the RMSE remains stable whereas SNR is further increasing. Such circumstances are shown in the graph on the lines with fixed I1 and I2 equal to 8, 10 and 12. These three lines performs no obvious differences from simulated results. Moreover, to achieve better result in higher SNR environment, the only method is increasing I1 to obtain larger resolution.

5.3.2 Comparison with Existed Methods

The existed methods to estimate the frequency of a real sinusoidal signal is either performing the window functions in time domain before Fourier analysis or using Matrix Pencil Method. Comparing with existed algorithms, we then demonstrate the advantages in refined estimator for real sinusoidal model. In the first part, we only use Parzen window as the reference, as Parzen reduce the more spectral leakage compared with most of other window functions. [22] Figure 5.5 shows the situation when f is small at 0.0125. In this

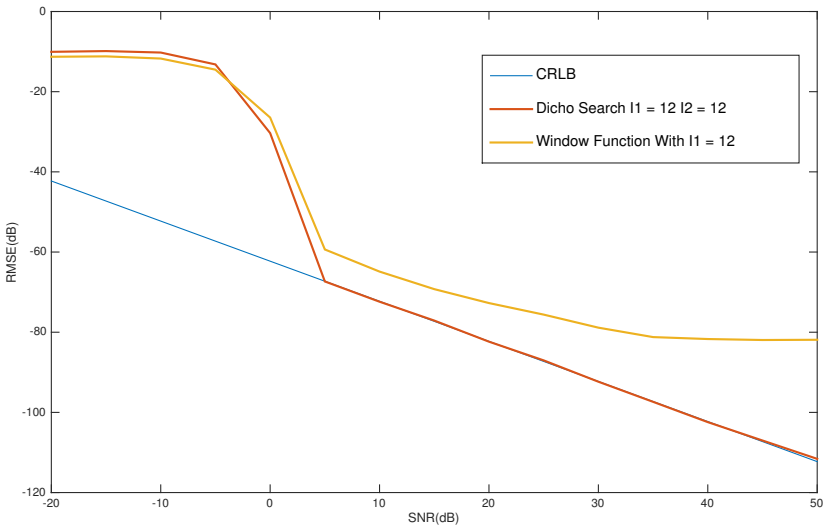

Figure 5.5: Comparison with Window Function @ $f = 0.0125$

case, window function shows even worse results when SNR is larger than 30dB due to main-lobe interference of two exponential signals. It is the trade-off from using window function, as it increase the bandwidth of main lobe at the same moment reduce the amplitude of side lobe to reduce the spectral leakage. When the increased bandwidth overlaps the true frequency from the sinc function in negative part, the overall performance is degraded. On the other hand, the refined estimator for real sinusoidal signal works perfectly without being influenced by small frequency, following with CRLB closely. If we modify

the frequency to 0.125 to ensure no effects coming from main-lobe interference, window function still works unsatisfactorily comparing with refined estimator, shown in Figure 56.

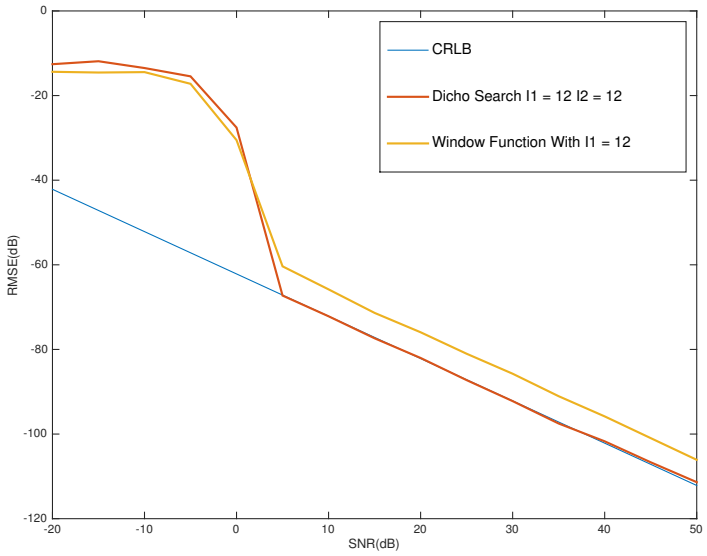

Figure 5.6: Comparison with Window Function @ $f = 0.125$

There is still an indispensable gap between RMSE for window function and CRLB. The reason is that the increased bandwidth flatten the peak in the maximum bin. The Gaussian noise induces more effects, thus the error is increased. Meanwhile, the refined estimator sits on the CRLB as SNR is increasing. Overall, the refined estimator results in better performance in each case comparing with window functions.

The simulation results are also compared with Matrix Pencil Method, which is shown in

Figure 5.7. From the graph, the refined algorithm behaves similar with Matrix Pencil,

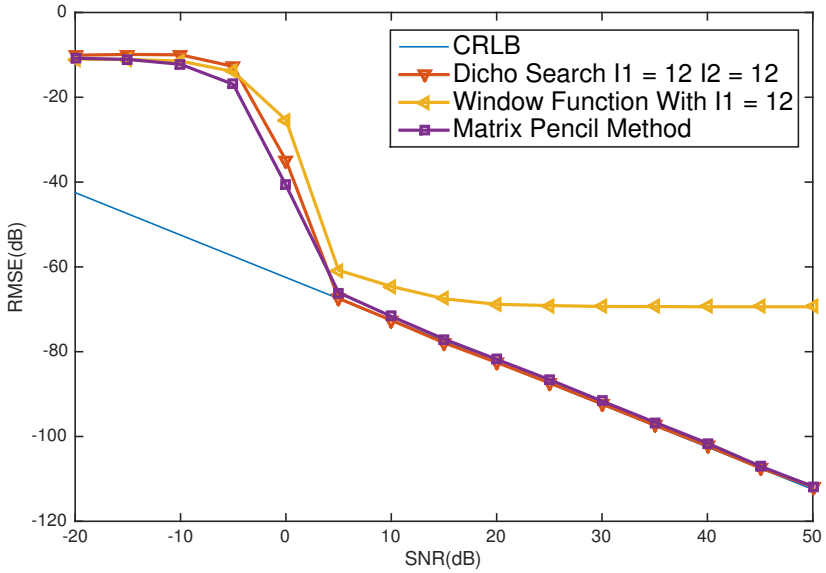

Figure 5.7: Comparison with Existed Methods @ $f = 0.0125$

as they are both accurate enough and eliminate the problems in spectral leakage and lack of resolution. From the enlarged view of the graph, shown as Figure 5.8, the refined algorithm is still better than Matrix Pencil and follows closer to the CRLB, although the deviation is not obvious.

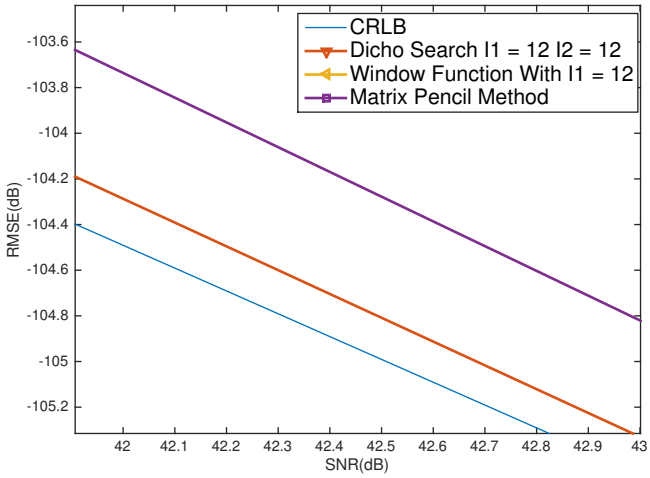

Figure 5.8: Enlarged View of Comparison @ $f = 0.0125$

5.4 Computational Complexity Analysis

Comparing with other algorithms in time domain, refined dichotomous algorithm has an obvious advantage in reducing the computational complexity. For other algorithms performing SVD calculations in time domain, the matrix inversion process consumes large amount of computational resources, related to $(O(N^3))$[27] calculations. On the other hand, the refined dichotomous searching algorithm based on AMDS is more efficient in reducing the number of calculations, as most calculations are based on FFT algorithm, with calculations of $O(N \log_2 N)$. For simplicity, we only take number of FFTs into account to estimate the overall computations.

In internal AMDS, the algorithm initially makes a coarse estimation with a FFT and changes the relevant maximum bin with a DFT. Then in refining iterations, it calculates a DFT in each cycle. Thus, AMDS consumes $(O(N \log_2 N)$ computations for one cycle with I1 iterations. In external leakage eliminating iteration process, the algorithm calls I2 times of AMDS functions. Thus, total computations are represented as $O(I2Nlog_2N)$ approximately. Therefore from the equation, I1 generates small effects in increasing computational pressure compared with I2. In simulated results, we use this algorithm to

estimate a signal with 1000 samples. We work on Matlab programme with 1000 times estimation for single I1&I2 pair to explore on the computational pressure. The result is shown below as table 5.1.

Comparing with existed algorithms including Matrix Pencil and Window Functions,

I1-I2	2	4	6	8	10	12
2	0.646	1.270	1.904	2.593	3.212	3.767
4	0.885	1.726	2.565	3.427	4.253	5.110
6	1.103	2.177	3.243	4.306	5.383	6.434
8	1.342	2.616	3.897	5.190	6.454	7.741
10	1.533	3.052	4.559	6.092	7.567	9.260
12	1.770	3.497	5.540	7.248	8.671	10.852

Table 5.1: Computational Time vs Various I1&I2 (unit: sec/1000times)

the result is shown as Figure 5.9. From the graph, although adding external iterations

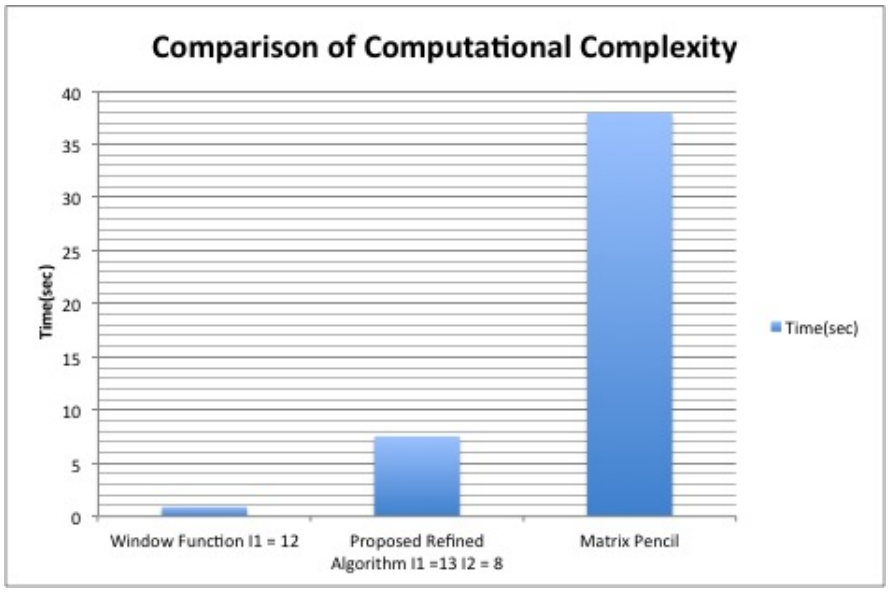

Figure 5.9: Comparison of Computational Complexity

$I2$ increases the overall computational time opposite to window functions, the efficiency is still satisfying compared with Matrix Pencil. For sufficient I1&I2 are provided as 12 and 8 respectively, the refined algorithm obtains accurate result following with CRLB for adequate SNR situations. It only costs about 0.07 second per estimation, which makes it more suitable for fast frequency tracking in smart grid with 82% less computational time comparing with Matrix Pencil method. Although window functions consume even less time, they sacrifice the overall estimating accuracy and are ineligible to perform as an accurate frequency estimator.

Chapter 6

Conclusion

6.1 Summary for the whole thesis

For ***existed frequency estimators used for a real sinusoid***, they are divided into:

1. Non-MLE algorithms: Estimating in time domain, such as using subspace methods.
2. MLE algorithms: Estimating in frequency domain, such as using Fourier Transformation.

The *estimating error in Non-MLE algorithms* is caused by:

1. Additive White Gaussian Noise: Estimating variance follows with CRLB.

The *estimating error in MLE algorithms* is caused by:

1. Additive White Gaussian Noise: Estimating variance follows with CRLB.
2. Lack of resolution: Resolving by interpolations and estimating variance follows with $\frac{\delta^2}{12}$
3. Spectral leakage effect: Estimating variance follows with amplitude of spectral leakage

Note that the overall estimating variance depends on the maximum value of each deviations. The mentioned non-MLE algorithm is Matrix Pencil and the mentioned MLE algorithm is window functions. The Matrix Pencil has:

1. **Advantages**: Sufficient accuracy following with CRLB.

2. **Disadvantages**: Complex computations and slow response which is not suitable for fast frequency tracking for the smart grid.

The window function with interpolations has:

1. **Advantages**: Simple computations and fast response.

2. **Disadvantages**: Low accuracy due to increased bandwidth, which is not suitable for an accurate frequency estimator.

For the facts of the refined algorithm for frequency estimation of a real sinusoid:

1. It is based on the existed efficient interpolation algorithm called Aboutanios's Modified Dichotomous Search to solve lack of resolution.

2. It adds external iterations to calculate and reduce the spectral leakage effect to eliminate the bias from the result.

From the simulated result, it has advantages in:

1. Outstanding accuracy which RMSE exactly follows CRLB for most of frequencies and initial phase shift with sufficient I1 and I2.

2. Efficient in computational complexity and providing the estimation with fast response.

It may still improve in the future in:

1. Improving the performance at extreme small frequencies.

6.2 Conclusion

In this thesis report, the author demonstrated the refined frequency estimator using for a real sinusoidal signal with additive white Gaussian noise, which is suitable for fast frequency tracking in smart grid. The refined estimator considers and eliminates the spectral leakage, developed from the modified dichotomous searching algorithm by Aboutanios. The refined method iteratively estimates the frequency by subtracting the leakage from time-domain signal combining with existed dichotomous interpolation scheme. Simulated results showed the outstanding performance as RMSE with sufficient iterations sit on CRLB closely. Comparing with existed methods, the refined methods provide the satisfying accuracy as well as reduce the required computational complexity to a reasonable level, although the performance for extreme small frequencies is degraded.

6.3 Future Works

1. Following with the simulating result, the refined frequency estimation algorithm should be tested on the frequency tracking system for a real smart grid. These tests directly reflect the accurate behaviours on suitability, stability and accuracy.

2. From Figure 5.2, the performance of refined algorithm is degraded at extreme small frequency. Thus, another future approach is to modify the refined algorithm to increase the accuracy at small frequencies.

Bibliography

[1] O. Vainio and S. Ovaska, Digital filtering for robust 50/60 Hz zero-crossing detecters, *IEEE Trans. Instrum. Meas.*, vol. 45, no. 2, pp. 426430, 2001.

[2] L. G. B. Barbosa Rolim, Jr., D. R. Rodrigues da Costa, and M. Aredes, Analysis and software implementation of a robust synchronizing PLL circuit based on the PQ theory, *IEEE Trans. Ind. Electron.*, vol. 53, no. 6, pp. 19191926, 2006.

[3] Y. Xia, S. C. Douglas, and D. P. Mandic, "Adaptive frequency estimation in smart grid applications", *IEEE signal processing magazine*, 1053-5888, page 44-54, 2012.

[4] P. Stoica and R. L. Moses, *Introduction to Spectral Analysis*, Prentice Hall, Upper Saddle River, New Jersey, 1997.

[5] R. Roy and T. Kailath, ESPRIT - Estimation of signal parameters via rotational invariance techniques, *IEEE Transactions on Acoustics, Speech, and Signal Processing*, vol. 37, no. 7, pp. 984995, 1989.

[6] Y. Hua and T. K. Sarkar, Matrix pencil method for estimating parameters of exponentially damped/undamped sinusoids in noise, IEEE Transactions on Acoustics, Speech, and Signal Processing, vol. 38, no. 5, pp. 814824, 1990.

[7] Y. Lin, P. Hodgkinson, M. Ernst and A. Pines, "A novel detection-estimation scheme for noisy nmr signals: applications to delayed acquisition data", *Journal of magnetic resonance*, vol 128, pp. 30-41, 1997.

[8] Y. V. Zakharov and T. C. Tozer, "Frequency estimator with dichotomoussearch of periodogram peak",*Electron. Lett.*, vol. 35, pp. 1608-1609, 1999.

[9] E Aboutanios, "A modified dichotomous search frequency estimator", *Signal Processing Letters*, IEEE 11 (2), 186-188, 2004

[10] F.J. Harris, On the use of windows for harmonic analysis with the discrete Fourier transform, *Proceedings of the IEEE*, vol. 66, no. 1, pp. 5183, 1978.

[11] K. Duda, L.B. Magalas, M. Majewski, and T.P. Zielinski, DFT-based estimation of damped oscillation parameters in low-frequency mechanical spectroscopy, *IEEE Transactions on Instrumentation and Measurement*, vol. 60, no. 11, pp. 3608 3618, 2011.

[12] E. Aboutanios, "Estimation of the Frequency and Decay Factor of a Decaying Exponential in Noise", *Signal Processing, IEEE Transactions*, vol. 58, issue 2, page 501-509, 2009.

[13] L.C. Lucien, *Maximum Likelihood an Introduction*, ISI Review, 1990.

[14] E. Aboutanios, "Estimating the Parameters of Sinusoids and Decaying Sinusoids in Noise", *IEEE Instrumentation & Measurement Magazine*, page: 1094-6969, 2011.

[15] E. Arthur ed, *Tables of Integral Transforms*, New Your: McGraw-Hill, 1954.

[16] D. Kammler, *A First Course in Fourier Analysis*, Prentice Hall, ISBN 0-13-578782-3,2000.

[17] D. C. Rife and R. R. Boorstyn, "Single tone parameter estimation from discrete-time observations," *IEEE Trans. Inform. Theory*, vol. IT-20, pp.591-598, 1974.

[18] S. M. Kay, *Modern Spectral Estimation:Theory and Applications*, Englewood Cliffs, NJ: Prentice-Hall, 1988.

[19] P. Stoica, H. Li and J. Li, "Amplitude estimation of sinusoidal signals: Survey, new results, and an application", *IEEE Trans. Signal Process.*, 48 (2), 338-352, 2000.

[20] D. Belega, D. Dallet and D. Slepicka, "Accurate amplitude estimation of harmonic components of incoherently sampled signals in the frequency domain", *IEEE Trans. Instrum. Meas.*, 59 (5), 1158-1166, 2010.

[21] R.Curtis, *Microsound*, MIT Press, ISBN 0-262-18215-7, 2002.

[22] F. J. Harris, "On the use of Windows for Harmonic Analysis with the Discrete Fourier Transform", *Proc. IEEE*, vol.66, pp. 51-83, 1978.

[23] K.Toraichi, M.Kamada, S.Itahashi and R.Mori, "Window functions represented by B-spline functions", *Acoustics, Speech and Signal Processing, IEEE Transactions*, vol. 37, issue. 1, 1989.

[24] H.B.Cuny, I.J.Schoenberg, "On Polya frequency functions. IV. The fundamental spline functions and their limits", *J. dAnalysC Math.*, vol.17, pp.71-107, 1966.

[25] J. O. Smith III, *Spectral Audio Signal Processing*, Center for Computer Research in Music and Acoustics (CCRMA), Department of Music, Stanford University, 2010.

[26] E. Aboutanios, Frequency estimation for low earth orbit satellites, Ph.D. thesis, Univ. Technology, Sydney, Australia, 2002.

[27] R. O. Schmidt, Multiple emitter location and signal parameter estimation, *IEEE Trans. Antennas Propagat.*, vol. 34, pp. 276280, Mar. 1986.